Simultaneous Lightwave Information and Power Transfer (SLIPT)

Panagiotis D. Diamantoulakis, *Member, IEEE,* George K. Karagiannidis, *Fellow, IEEE,* and Zhiguo Ding, *Senior Member, IEEE*

***Abstract*—We present the concept of simultaneous lightwave information and power transfer (SLIPT). Specifically, we propose novel and fundamental SLIPT strategies, which can be optimized and implemented in visible light or infrared communication systems, equipped with a simple solar panel at the receiver. These strategies are performed at the transmitter or at the receiver, or at both sides, and are named as *adjusting transmission*, *adjusting reception*, and *coordinated adjustment of transmission and reception*. Furthermore, they affect the maximum value of harvested energy, information rate, and signal-to-noise plus interference ratio. Computer simulations reveal that the proposed strategies considerably increase the harvested energy, compared to SLIPT with fixed policies.**

I. Introduction

THE era of internet-of-things (IoT) opens up the opportunity for a number of promising applications in smart buildings, health monitoring, and predictive maintenance. In the context of wireless access to IoT devices, radio frequency (RF) technology is the main enabler. Furthermore, the exponential growth in the data traffic puts tremendous pressure on the existing global telecommunication networks and the expectations from the fifth generation (5G) of wireless networks. Also, it is remarkable that most of the data consumption/generation, which are related to IoT applications, occurs in indoor environments [1]. Motivated by this, optical wireless communications (OWC), and especially visible light communications (VLC) or infrared communications (IRC), have been recognized as promising alternative/complementary technologies to RF, in order to provide access to IoT devices in indoor applications [1]. Consequently, VLC/IRC are envisioned to be used in a vast number of scenarios, such as in offices, commercial centers, airports, hospitals, industrial environments, in-flight internet etc.

The data rates reported for indoor VLC/IRC networking are much higher than those achieved by WiFi, especially when client and server are closely located. Apart from the very high data rates [2], the advantages of OWC technologies include: i) increase of available bandwidth, ii) easy bandwidth reuse, iii) increase of energy efficiency and considerable energy savings, iv) no RF contamination, and v) free from RF interference. Moreover, nowadays, light emitting diodes (LEDs) and photodetectors (PDs) tend to be considerably cheaper than their RF counterparts, while the cost-efficiency is further improved due to the potential use of the existing lighting infrastructure [3]–[5].

Due to the strong dependence of the IoT on wireless access, their applications are constrained by the finite battery capacity of the involved devices [6]. Therefore, energy harvesting (EH), which refers to harnessing energy from the environment or other sources and converting to electrical energy, is a critical part of the operation and maintenance of the IoT devices [7]. Energy harvesting is regarded as a disruptive technological paradigm to prolong the lifetime of energy-constrained wireless networks, which apart from offering a promising solution for energy-sustainability of wireless nodes [7], [8], it also reduces the operational expenses (OPEX) [6]. However, the main disadvantage of traditional EH methods is that they rely on natural resources, such as solar and wind, which are uncontrollable. For this reason, harvesting energy from sources, that intentionally generate an electromagnetic (EM) field, seems to be an interesting alternative. The major wireless charging techniques are inductive coupling, magnetic resonance coupling, RF radiation, and light waves, with the first two being appropriate only in near-field power transfer [9].

An important challenge associated with the wireless powered systems is the reduction of the unwanted interference, EM pollution (e.g., light pollution [10]), and exposure of people and other living things to potentially injurious EM radiation, which calls for conscious utilization of the radiated energy [11]. This can be achieved by unifying the information and energy transmission, which is the basis of simultaneous wireless information and power transfer (SWIPT) [12], [13]. Note that SWIPT, when properly optimized, can result in significant gains in terms of spectral efficiency, time delay, energy consumption, and interference management, by superposing information and power transfer. However, this approach, calls for the redesign of existing wireless networks, which has been initally investigated by the pioneer works [14] and [15]. For example, when the aim is to harvest energy from RF signals,

Manuscript received XXXXXX; revised XXXXXX; accepted XXXXXX. Date of publication XXXXXX; date of current version XXXXXX. The work of Z. Ding was supported by the UK EPSRC under grant number EP/N005597/1 and by H2020-MSCA-RISE-2015 under grant number 690750. Part of this work has been presented in IEEE Global Communications Conference (GLOBECOM), Singapore, May 2017.

P. D. Diamantoulakis and G. K. Karagiannidis are with the Department of Electrical and Computer Engineering, Aristotle University of Thessaloniki, 54 124, Thessaloniki, Greece (e-mails: {padiaman,geokarag}@auth.gr).

Z. Ding is with the School of Computing and Communications, Lancaster University, LA1 4WA, UK (e-mail: z.ding@lancaster.ac.uk).

Color versions of one or more of the figures in this paper are available online at http://ieeexplore.ieee.org

Digital Object Identifier XX.XXXX/TGCN.201X.XXXXXX

This article has been accepted for publication in a future issue of this journal, but has not been fully edited. Content may change prior to final publication. Citation information: DOI 10.1109/TGCN.2018.2818325, IEEE Transactions on Green Communications and Networking

which also transfer information by using single-antenna nodes, two fundamental receiver structures have been proposed, named: *power-splitting (PS)* [15], and *time-switching (TSw)* [15], [16]. PS is based on the splitting of the signal's power into two streams, while in TSw, using a switching key at the receiver, for a portion of time the received signal is used solely for energy harvesting. Note that these strategies create an interesting trade-off between the the rate and the harvested energy, which is investigated in [17]–[19].

A. Related Research and Motivation

Although RF based wireless power transfer is a well investigated topic in the last years [20], optical wireless power transfer is a new topic and only a few works have been reported so far in the open literature. In the fundamental paper of Fakidis et. al. [21], the visible and infrared parts of the electromagnetic (EM) spectrum was used for OWPT, through laser or LEDs at the transmitter and solar cells at the receiver side. Also, in [22] and [23] energy harvesting was performed, by using the existing lighting fixtures for indoor IoT applications. Moreover, in [9], distributed laser charging is discussed, with the main emphasis being given on the benefits of lightwave power transfer, compared to the other three major wireless charging techniques, i.e., inductive coupling, magnetic resonance coupling, and microwave radiation. Furthermore, in [24], a hybrid VLC-RF system with light energy harvesting over the downlink is considered. The secrecy outage performance of the RF-based uplink is investigated, while considering the randomness of the locations of the legitimate receiver and the eavesdropper.

Regarding the simultaneous optical wireless information and power transfer, in [25] the sum rate maximization problem has been solved in a downlink VLC system. However, in this paper the utilized energy harvesting model does not correspond to that of the solar panel, where only the direct current (DC) component of the modulated light can be used for energy harvesting, in contrast to the alternating current (AC) component, which carries the information. The separation of the DC and AC components was efficiently achieved by the self-powered solar panel receiver, proposed in [26], [27], where it was proved that the use of the solar panel for communication does not limit its energy harvesting capabilities. Thus, the utilization of the power-splitting in [28] reduces the EH efficiency. Moreover, in [28] an oversimplified energy harvesting model was used, assuming that the harvested energy is linearly proportional to the received optical power, while an optimization of the splitting technique was not presented. In [29], the implementation of a solar panel receiver prototype was reported, which is able to gather energy and receive data simultaneously. Also, the field-of view (FoV) of the photodetector (PD) was considered in the model analysis. Furthermore, in [30], [31], a dual-hop hybrid VLC/RF communication system is considered, in order to extend the coverage. In these papers, besides detecting the information over the VLC link, the relay is also able to harvest energy from the first-hop VLC link, by extracting the DC component of the received optical signal. This energy can be used to re-transmit the data to a mobile terminal over the second-hop RF link. Also, in [30] the proposed hybrid system was optimized, in terms of data rate maximization, while in [31] the packet loss probability was evaluated.

Taking into account the aforementioned research, it is evident that the theoretical investigation of simultaneous information and power transfer using lightwave technology is still in its infancy. More specifically, appropriate strategies are required to increase the efficiency, as well as an optimization framework that takes into account and regulates the trade-off between the harvested energy and the communication performance. It is noted that this dual-purpose exploitation of light is fundamentally different to the corresponding use of RF signals, due to divergent channels characteristics, transmission/reception devices and EH model, among others.

B. Contribution

In this paper, we present -for first time- a framework for the simultaneous optical wireless information and power transfer, called from now on as *simultaneous lightwave information and power transfer (SLIPT)*. More specifically, the contribution can be summarized as follows:

- We propose novel and fundamental strategies in order to increase the feasibility and efficiency of SLIPT, when a solar panel-based receiver is used. These strategies are performed at the transmitter or at the receiver, or at both sides, named *adjusting transmission*, *adjusting reception*, and *coordinated adjustment of transmission and reception*.
- Regarding adjusting transmission two policies are proposed:
  i. *Time-splitting (TS)*, which is based on the separation of the transmission block in two distinct phases, where in each of them the main focus is either on communication or energy transfer. Although inspired by TSw in RF SWIPT [15], SLIPT TS presents significant differences compared to TSw, mainly due to the differentation of the utilized RF and lightwave technologies. More specifically, TS does not use a switching key and is referred to the adjustment of the transmission parameters, i.e., the DC bias and peak amplitude of the transmitted optical signal at each phase. Also, the separation of the DC and AC components at the receiver is achieved in parallel, by using an inductor and a capacitor at the EH and information decoding branch, respectively [27]. This justifies the utilization of the term "splitting" instead of "switching". Moreover, in TSw, one of the two phases is dedicated solely to information transmission, while during this phase the harvested energy is zero. This is not the case in TS, where energy can be harvested in both phases due to the DC bias, which is always higher than zero.
  ii. *Time-splitting with DC bias optimization*, which is a generalization of TS. In contrast to SWIPT, where the TS strategy and adjustment of the related parameters takes place at the receiver's side, TS in SLIPT refers to

This article has been accepted for publication in a future issue of this journal, but has not been fully edited. Content may change prior to final publication. Citation information: DOI 10.1109/TGCN.2018.2818325, IEEE Transactions on Green Communications and Networking

the adaptation of specific parameters of the transmitted signal.

- Regarding adjusting reception, the *field-of-view (FoV) adjustment* policy is proposed.
- For the coordinated adjustment of transmission and reception strategy, we propose the joint optimization of the former policies at both transmitter and receiver.
- In order to balance the fundamental trade-off between harvested energy and quality-of-service (QoS) (e.g. data rate and signal-to-noise plus interference ratio (SINR)), two optimization problems are formulated and optimally solved, which aim at maximizing the harvested energy, while achieving the required user's QoS.
- Finally, simulation results are provided to compare the proposed optimal strategies with the fixed policies and verify their effectiveness.

It is highlighted that, although the proposed strategies are quite general and can be applied in different applications, the provided analysis and the simulation results focus on indoor applications through VLC or IRC.

C. Structure

The rest of the paper is organized as follows. Section II describes the considered communication and energy harvesting model. Section III introduces the SLIPT strategies. The optimization problem of harvested energy maximization is formulated and solved in section IV. Section V presents and discusses the simulation results and finally, section VI concludes the paper with some remarks.

II. System and Channel Model

We consider the downlink transmission of a SLIPT VLC/IRC system, consisting of one LED and a single user. We also assume that the user is equipped with the functionality of energy harvesting. The SLIPT transmitter/receiver design is shown in Fig. 1, while the SLIPT downlink communication is depicted in Fig. 2.

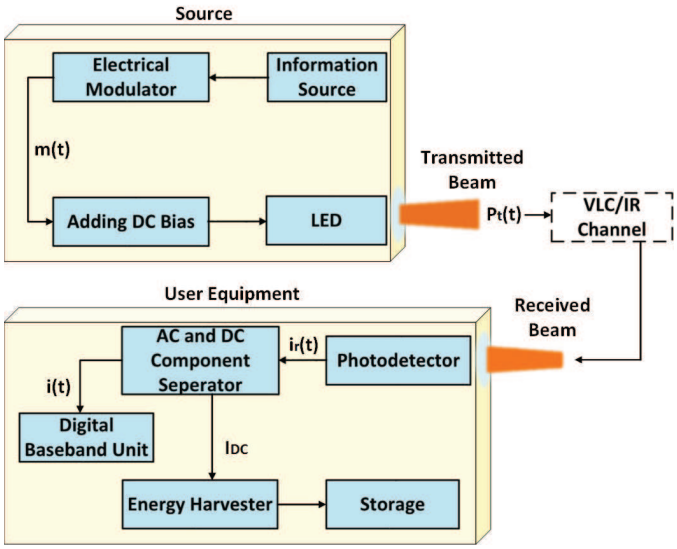

Fig. 1. SLIPT transceiver design

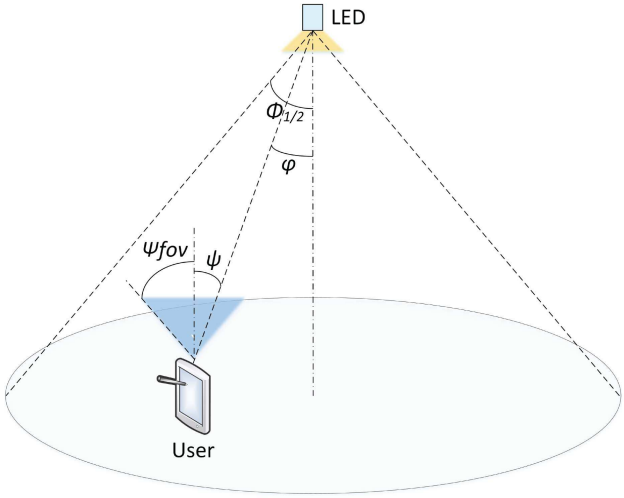

Fig. 2. A SLIPT downlink communication system

A. Optical Wireless Transmission

Let $m(t)$ denote the modulated electrical signal that corresponds to the bit stream from the information source. A DC bias B is added to $m(t)$ to ensure that the resulting signal is non-negative, before being used to modulate the optical intensity of the LED and regulate the LED in the proper operation mode. The transmitted optical signal from the LED is [30]

$$P_t(t) = P_{\mathrm{LED}}[B + m(t)], \tag{1}$$

where P_{LED} is the LED power per unit (in W/A) of electrical current $B + m(t)$. The electrical signal varies around the DC bias $B \in [I_{\mathrm{L}}, I_{\mathrm{H}}]$ with peak amplitude A, where I_{L} is the minimum and I_H is the maximum input bias currents, correspondingly. In order to avoid clipping distortion by the nonlinearity of the LED, by restraining the input electrical signal to the LED within the linear region of the LED operation, the following limitation is induced

$$A \leq \min(B - I_{\mathrm{L}}, I_{\mathrm{H}} - B). \tag{2}$$

B. Channel Model

The channel gain is given by [32]–[34]

$$h = \frac{L_{\mathrm{r}}}{d^2} R_0(\varphi) T_{\mathrm{s}}(\psi) g(\psi) \cos(\psi), \tag{3}$$

where φ is the irradiance angle, ψ is the incidence angle, L_r is the physical area of the photo-detector, d is the transmission distance from the LED to the illuminated surface of the photo-detector, $T_{\mathrm{s}}(\psi)$ is the gain of the optical filter and $g(\psi)$ represents the gain of the optical concentrator, given by [32], [34]

$$g(\psi) = \begin{cases} \frac{\rho^2}{\sin^2(\Psi_{\mathrm{fov}})}, & 0 \leq \psi \leq \Psi_{\mathrm{fov}}, \\ 0, & \psi > \Psi_{\mathrm{fov}}, \end{cases} \tag{4}$$

with ρ and Ψ_{fov} being the refractive index and FoV, respectively. From (4), we see that as the FoV is reduced, the

gain within the FoV is increased. Also in (3), $R_0(\varphi)$ is the Lambertian radiant intensity of the LED, given by

$$R_0(\varphi) = \frac{\xi + 1}{2\pi} \cos^{\xi} \varphi, \tag{5}$$

where ξ is the order of Lambertian emission, and is given by the semi-angle at half illuminance of the LED, $\Phi_{1/2}$, as

$$\xi = -\frac{1}{\log_2(\cos(\Phi_{1/2}))}. \tag{6}$$

For example, $\Phi_{1/2} = 60$ deg corresponds to $\xi = 1$. From (3) we can observe that if d and $R_0(\varphi)$ are fixed, the most effective way to increase h are to increase the detector area $L_{\rm r}$ and increase the concentrator gain, e.g., by decreasing the FoV.

C. Received Electrical SINR

The electrical current $i_r(t)$ at the output of the PD can be written as

$$i_r = \eta(hP_t(t) + P_o) + n(t) = I_{\rm DC}(t) + i(t) + n(t), \tag{7}$$

where η is the photo-detector responsivity in A/W, P_o is the received optical signal from other sources, e.g. other neighboring LEDs, $I_{\rm DC}$ is the DC component, $i(t)$ is the AC component, and $n(t)$ is the additive white Gaussian noise (AWGN), which is created from background shot noise and thermal noise.

The AC component $i(t)$ is composed of two terms, i.e.,

$$i(t) = i_1(t) + i_2(t), \tag{8}$$

where

$$i_1(t) = \eta h P_{\rm LED} m(t) \tag{9}$$

is due to the dedicated LED, and $i_2(t)$ is due to other interfering sources. Thus, the received SINR can be written as

$$\gamma = \frac{(\eta h P_{\rm LED} A)^2}{P_{\rm I} + \sigma^2}, \tag{10}$$

where σ^2 is the noise power and $P_{\rm I}$ is the electrical power of the received interference.

D. Energy Harvesting Model

As it has already been mentioned the photocurrent consists of both the DC and AC signals. In order to perform energy harvesting, the DC component is blocked by a capacitor and passes through the energy harvesting branch [26]. The harvested energy is given by [35]

$$E = f I_{\rm DC} V_{\rm oc}, \tag{11}$$

with f being the fill factor [35] and

$$I_{\rm DC} = I_1 + I_2 \tag{12}$$

being the DC component of the output current, where

$$I_1 = \eta h_n P_{\rm LED} B \tag{13}$$

is due to the dedicated LED, while I_2 is due to different light sources, e.g. neighboring LEDs. Also, $V_{\rm oc}$ is

$$V_{\rm oc} = V_t \ln(1 + \frac{I_{\rm DC}}{I_0}), \tag{14}$$

where V_t is the thermal voltage and I_0 is the dark saturation current of the PD.

III. SLIPT Strategies

In this section, we propose fundamental SLIPT strategies for use in VLC/IRC.

A. Adjusting Transmission

First, we introduce two policies for the adjusting transmission strategy, named *time-splitting (TS)* and *TS with DC bias optimization*.

1) TS: According to the TS policy the received optical signal is used for a portion of time solely for energy harvesting, instead of decoding. During this period of time the LED transmits by using the maximum DC bias, in order to maximize the harvested energy by the receiver.

Let $T_{\rm tot}$ denote the block transmission time, which is measured in seconds. Also, τ (unitless value) is the portion of time that is allocated solely to the first phase, in which information transmission is enabled. Thus, the duration of the first phase in seconds is $T = \tau T_{\rm tot}$. Without loss of generality, we assume that $T_{\rm tot} = 1$ second in the sequel. The two distinct phases are discussed in detail below.

Phase 1: The AC component of the received signal is used for information decoding and the DC component for energy harvesting. Let A_1 and $B_1 \in [I_{\rm L}, I_{\rm H}]$ denote the peak amplitude of $m(t)$ and DC bias, respectively. During Phase 1, the aim is to maximize the received SINR, denoted by γ_1. Since SINR is an increasing function with respect to A_1, then A_1 takes its maximum value, which, considering (2) is given by

$$A_1 = \frac{I_{\rm H} - I_{\rm L}}{2} \tag{15}$$

and similarly,

$$B_1 = \frac{I_{\rm H} + I_{\rm L}}{2}. \tag{16}$$

The duration of this phase $T \in [0, 1\,\text{second}]$ can be optimized according to the QoS requirements. For a specific value of T, the amount of harvested energy is given by

$$\begin{aligned} E_{\rm TS}^{[1]} = fT(\eta h P_{\rm LED} \frac{I_{\rm H} + I_{\rm L}}{2} + I_2) V_t \\ \times \ln(1 + \frac{\eta h P_{\rm LED} \frac{I_{\rm H} + I_{\rm L}}{2} + I_2}{I_0}). \end{aligned} \tag{17}$$

Phase 2: In the time period $1 - T$, the aim is to maximize the harvested energy, which is an increasing function with respect to B. Thus, during Phase 2 the transmitter eliminates the AC part and the and maximizes the DC bias, i.e., $A = 0$ and $B = I_{\rm H}$, with the SINR being $\gamma_2 = 0$, where A_2 and $B_2 \in [I_{\rm L}, I_{\rm H}]$ denote the values of A and B, respectively.

This article has been accepted for publication in a future issue of this journal, but has not been fully edited. Content may change prior to final publication. Citation information: DOI 10.1109/TGCN.2018.2818325, IEEE Transactions on Green Communications and Networking

TABLE I
PROPOSED STRATEGIES AND POLICIES

STRATEGY/Policy / Parameter	ADJUSTING TRANSMISSION		ADJUSTING RECEPTION	COORDINATED ADJUSTMENT OF TRANSMISSION & RECEPTION	
	Time-splitting	**Time-spliting with DC bias optimization**	**Adjustment of the FoV**	**Time-splitting with tunable FoV**	**Time-splitting with DC bias optimization and tunable FoV**
Time dedicated solely to energy harvesting $(1-T)$	Dynamic $T \in (0,1]$	Dynamic $T \in (0,1]$	Fixed $T=1$	Dynamic $T \in (0,1]$	Dynamic $T \in (0,1]$
DC Bias (B)	Fixed in each phase $B_1 = \frac{I_{\mathrm{H}}+I_{\mathrm{L}}}{2}$, $B_2 = I_{\mathrm{H}}$	Dynamic in the 1-st, fixed in the 2-nd phase $B_1 \in [I_{\mathrm{L}}, I_{\mathrm{H}}]$, $B_2 = I_{\mathrm{H}}$	Fixed $B_1 = B_2 = B$	Fixed in each phase $B_1 = \frac{I_{\mathrm{H}}+I_{\mathrm{L}}}{2}$, $B_2 = I_{\mathrm{H}}$	Dynamic in the 1-st, fixed in the 2-nd phase $B_1 \in [I_{\mathrm{L}}, I_{\mathrm{H}}]$, $B_2 = I_{\mathrm{H}}$
Peak amplitude (A)	Fixed in each phase $A_1 = \frac{I_{\mathrm{H}}-I_{\mathrm{L}}}{2}$, $A_2 = 0$	Dynamic in the 1-st, fixed in the 2-nd phase $A_1 \leq \min(B_1 - I_{\mathrm{L}}, I_{\mathrm{H}} - B_1)$, $A_2 = 0$	Fixed $A_1 = A_2 = A$	Fixed in each phase $A_1 = \frac{I_{\mathrm{H}}-I_{\mathrm{L}}}{2}$, $A_2 = 0$	Dynamic in the 1-st, fixed in the 2-nd phase $A_1 \leq \min(B_1 - I_{\mathrm{L}}, I_{\mathrm{H}} - B_1)$, $A_2 = 0$
Field of view (FoV)	Fixed	Fixed	Dynamic	Dynamic in each phase	Dynamic in each phase
SINR (γ)	Fixed in each phase $\gamma_1 = \frac{(\eta h P_{\mathrm{LED}}(I_{\mathrm{H}}-I_{\mathrm{L}}))^2}{4(P_{\mathrm{I}}+\sigma^2)}$, $\gamma_2 = 0$	Dynamic in the 1-st, fixed in the 2-nd phase $\gamma_1 = \frac{(\eta h P_{\mathrm{LED}} A_1)^2}{P_{\mathrm{I}}+\sigma^2}$, $\gamma_2 = 0$	Dynamic $\gamma = \frac{(\eta h P_{\mathrm{LED}} A)^2}{P_{\mathrm{I}}+\sigma^2}$	Dynamic in the 1-st, fixed in the 2-nd phase $\gamma_1 = \frac{(\eta h P_{\mathrm{LED}}(I_{\mathrm{H}}-I_{\mathrm{L}}))^2}{4(P_{\mathrm{I}}+\sigma^2)}$, $\gamma_2 = 0$	Dynamic in the 1-st, fixed in the 2-nd phase $\gamma_1 = \frac{(\eta h P_{\mathrm{LED}} A_1)^2}{P_{\mathrm{I}}+\sigma^2}$, $\gamma_2 = 0$
Harvested Energy (E)	$E = fT(\eta h P_{\mathrm{LED}} B_1 + I_2) V_t \times \ln(1 + \frac{\eta h P_{\mathrm{LED}} B_1 + I_2}{I_0}) + f(1-T)(\eta h P_{\mathrm{LED}} B_2 + I_2) V_t \times \ln(1 + \frac{\eta h P_{\mathrm{LED}} B_2 + I_2}{I_0})$				

Thus, the amount of harvested energy during this phase, is given by

$$E_{\mathrm{TS}}^{[2]} = f(1-T)(\eta h P_{\mathrm{LED}} I_{\mathrm{H}} + I_2) V_t \times \ln(1 + \frac{\eta h P_{\mathrm{LED}} I_{\mathrm{H}} + I_2}{I_0}). \quad (18)$$

Considering both phases, the total harvested energy is given by

$$E_{\mathrm{TS}} = E_{\mathrm{TS}}^{[1]} + E_{\mathrm{TS}}^{[2]}. \quad (19)$$

2) TS with DC Bias Optimization: This policy is a generalization of TS. During Phase 1, the DC bias is optimized in order to increase the harvested energy, while it simultaneously enables information transfer, i.e., $A_1 > 0$. In this case, the total harvested energy is given by

$$E_{\mathrm{TSBO}} = fT(\eta h P_{\mathrm{LED}} B_1 + I_2) V_t \times \ln(1 + \frac{\eta h P_{\mathrm{LED}} B_1 + I_2}{I_0}) + E_{\mathrm{TS}}^{[2]}. \quad (20)$$

B. Adjusting Reception

In this subsection, we propose the *adjustment of the field of view (FoV)* policy as a reception strategy, in order to balance the trade-off between harvested energy and SINR. The control of FoV is particularly important, especially when there are extra light sources in the serving area [36], e.g. neighboring LEDs that serve other users. For the practical and efficient implementation of this policy, electrically controllable liquid crystal (LC) lenses is a promising technology [37].

When the aim is to maximize the SINR, the FoV is tuned up to receive the beam of the dedicated LED only (if possible), in order to reduce the beam overlapping. This is achieved by tuning the FoV to the narrowest setting, that allows reception only from that LED. On the other hand, when the aim is to achieve a balance between SINR and harvested energy, a wider FoV setting could be selected.

For the sake of practicality, we assume that the SLIPT receiver has discrete FoV settings, i.e., $\Psi_{\mathrm{fov}} \in \{\Psi_{\mathrm{fov}}^{[1]}, .., \Psi_{\mathrm{fov}}^{[M]}\}$. Also, note that except for h, both P_{I} and I_2 are also discrete functions of Ψ_{fov}, i.e., $P_{\mathrm{I}} = P_{\mathrm{I}}(\Psi_{\mathrm{fov}})$ and $I_2 = I_2(\Psi_{\mathrm{fov}})$.

C. Coordinated Adjustment of Transmission and Reception

Considering (10), (19), and (20), it is revealed that both SINR and harvested energy -apart from A_1, B_1 and T- also depend on the selection of Ψ_{fov}, despite the utilized adjusting transmission technique. This dependence motivates the coordinated adjustment of transmission and reception, i.e. the coordination between the strategy III-A1 or III-A2 and III-B, which results in the following two policies, i.e.,

- Policy 1: TS with tunable FoV (III-A1 and III-B)
- Policy 2: TS with DC bias optimization and tunable FoV (III-A2 and III-B).

Note that in both policies, during Phase 2, where the aim is to maximize the harvested energy, the FoV setting that maximizes $E_{\mathrm{TS}}^{[2]}$ should be used. This is not necessarily the widest setting, because although it increases the received beams (if there are neighboring LEDs), it reduces $g(\psi)$. On the other hand, the preferable FoV setting during phase 1, denoted by $\Psi_{\mathrm{fov},1}$, cannot be straightforwardly determined, since it also depends on the required QoS.

This article has been accepted for publication in a future issue of this journal, but has not been fully edited. Content may change prior to final publication. Citation information: DOI 10.1109/TGCN.2018.2818325, IEEE Transactions on Green Communications and Networking

For clarity, the proposed strategies and policies are concluded in Table I.

IV. SLIPT Optimization

SLIPT induces a trade-off between harvested energy and QoS. In the present work, we focus on the coordinated adjustment of transmission and reception strategy, which can be considered as a generalization of the other SLIPT strategies. Regarding the QoS, two different criteria are taken into account, namely SINR and information rate. More specifically, since only Phase 1 is used for information transmission (with duration $T \leq 1$ second), a lower bound of the achievable rate in bits/second/Hz, within a block with $T_{\rm tot} = 1$ second, can be expressed as [38]

$$R = T \log_2 \left(1 + \frac{e}{2\pi}\gamma_1\right). \tag{21}$$

Note that the combination of TS with DC bias optimization and/or adjustment of the FoV creates an interesting trade-off among the rate, the SINR, and the harvested energy. Thus, given a harvested energy requirement, increasing the SINR might lead to a reduction of the rate and vise versa. Also, for a specific SINR value, a different rate-energy region is created. For example, in applications with low rate requirements, considering solely the rate-harvested energy region, might lead to selection of a point that does not satisfy the practical SINR requirement to enable detection. In that case, the optimal solution belongs in a different rate-energy subregion, that corresponds to a different SINR value, for which, given the harvested energy requirement, the rate might be lower. This is because, in order to satisfy the SINR requirement, B and/or FoV are decreased, while the duration of the second phase $(1-T)$ is increased, such as to harvest the same energy, which is turn might lead to a reduction of the rate. Specifically, the achievable rate-energy-SINR region can be written as (22) and (23), for Policy 1 and Policy 2, respectively.

Next, we seek to balance the aforementioned trade-off among the harvested energy, the achievable rate, and the SINR, by maximizing the harvested energy, while achieving the required information rate and SINR for the two policies of coordinated adjustment of transmission and reception. The corresponding optimization problems are formulated and optimally solved in the next subsections.

A. Time-Splitting with Tunable FoV

When the time-splitting with tunable FoV is used, the corresponding optimization problem can be expressed as

$$\begin{aligned} \underset{T,\Psi_{\rm fov,1}}{\textbf{max}} \quad & E_{\rm TS} \\ \textbf{s.t.} \quad & {\rm C}_1 : R \geq R_{\rm th}, \\ & {\rm C}_2 : \gamma_1 \geq \gamma_{\rm th}, \\ & {\rm C}_3 : 0 \leq T \leq 1, \\ & {\rm C}_4 : \Psi_{\rm fov,1} \in \{\Psi_{\rm fov}^{[1]}, .., \Psi_{\rm fov}^{[M]}\}, \end{aligned} \tag{24}$$

where $R_{\rm th}$ denotes the information rate and SINR threshold, respectively.

Theorem 1: The optimal value of T in (24) is given by

$$T^* = \frac{R_{\rm th}}{\log_2 \left(1 + \frac{e(\eta h P_{\rm LED}(I_{\rm H}-I_{\rm L}))^2}{8\pi(P_{\rm l}(\Psi^*_{\rm fov,1})+\sigma^2)}\right)}, \tag{25}$$

where $(\cdot)^*$ denotes optimality.

Proof: The optimization problem (24) is a combinatorial one. In order to find the optimal solution, all possible values of $\Psi_{\rm fov,1}$ have to be checked before selecting the value that maximizes the harvested energy, $E_{\rm TS}$, while satisfying the constraints ${\rm C}_1$, ${\rm C}_2$, and ${\rm C}_3$. For a specific value of $\Psi_{\rm fov,1}$, if

$$\frac{(\eta h P_{\rm LED}\frac{I_{\rm H}-I_{\rm L}}{2})^2}{P_{\rm l}(\Psi_{\rm fov,1}) + \sigma^2} < \gamma_{\rm th}, \tag{26}$$

then the optimization problem is infeasible, since ${\rm C}_2$ is not satisfied. Also, due to constraint ${\rm C}_1$, the following limitation is induced for T,

$$T \geq \frac{R_{\rm th}}{\log_2 \left(1 + \frac{e(\eta h P_{\rm LED}\frac{I_{\rm H}-I_{\rm L}}{2})^2}{2\pi(P_{\rm l}(\Psi_{\rm fov,1})+\sigma^2)}\right)}. \tag{27}$$

Moreover, the harvested energy is decreasing with respect to T. Thus, the optimal value of T is given by (25) and the proof is completed. ■

Note that if $T^* > 1$, the optimization problem in (24) is infeasible, due to ${\rm C}_3$.

B. Time-Splitting with DC Bias Optimization and Tunable FoV

When the time-splitting with DC Bias Optimization and tunable FoV is used, the corresponding optimization problem can be formulated as

$$\begin{aligned} \underset{B_1,A_1,T,\Psi_{\rm fov,1}}{\textbf{max}} \quad & E_{\rm TSBO} \\ \textbf{s.t.} \quad & {\rm C}_1 : R \geq R_{\rm th}, \\ & {\rm C}_2 : \gamma_1 \geq \gamma_{\rm th}, \\ & {\rm C}_3 : A_1 \leq \min(B_1 - I_{\rm L}, I_{\rm H} - B_1), \\ & {\rm C}_4 : 0 \leq T \leq 1, \\ & {\rm C}_5 : A_1 \geq 0, \\ & {\rm C}_6 : I_{\rm L} \leq B_1 \leq I_{\rm H}, \\ & {\rm C}_7 : \Psi_{\rm fov,1} \in \{\Psi_{\rm fov}^{[1]}, .., \Psi_{\rm fov}^{[M]}\}. \end{aligned} \tag{28}$$

Proposition 1: The optimal value of B in (28) belongs in the range $\left[\frac{I_{\rm H}+I_{\rm L}}{2}, I_{\rm H}\right]$.

Proof: The constraint ${\rm C}_3$ can be rewritten as

$${\rm C}_{3a} : A_1 \leq B_1 - I_{\rm L}, {\rm C}_{3b} : A_1 \leq I_{\rm H} - B_1. \tag{29}$$

For a specific value of B_1, only one of the constraints ${\rm C}_{3a}$ and ${\rm C}_{3b}$ is activated. Now, let assume that the optimal solution is

$$B_1^* < \frac{I_{\rm H} + I_{\rm L}}{2}, \tag{30}$$

for which all the constraints are satisfied. In this case, ${\rm C}_{3a}$ is activated. However, by setting

$$B_1 = \frac{I_{\rm H} + I_{\rm L}}{2}, \tag{31}$$

the objective function is increased, while the constraints are still satisfied. Thus, we can infer that that B_1^* is not optimal.

This article has been accepted for publication in a future issue of this journal, but has not been fully edited. Content may change prior to final publication. Citation information: DOI 10.1109/TGCN.2018.2818325, IEEE Transactions on Green Communications and Networking

$$\mathcal{C}_{\mathrm{R-E-}\gamma}^{\mathrm{TS}} \triangleq \bigcup_{T,\Psi_{\mathrm{fov},1}} \Bigg\{ (R', E'_{\mathrm{TS}}, \gamma'_1) : R' \leq T \log_2 \left(1 + \frac{(e\eta h P_{\mathrm{LED}} \frac{I_{\mathrm{H}}-I_{\mathrm{L}}}{2})^2}{2\pi \left(P_{\mathrm{I}}(\Psi_{\mathrm{fov},1}) + \sigma^2 \right)} \right), E'_{\mathrm{TS}} \leq fT(\eta h P_{\mathrm{LED}} \frac{I_{\mathrm{H}} + I_{\mathrm{L}}}{2} + I_2) V_t \times$$
$$\ln(1 + \frac{\eta h P_{\mathrm{LED}} \frac{I_{\mathrm{H}}+I_{\mathrm{L}}}{2} + I_2}{I_0}) + f(1-T)(\eta h P_{\mathrm{LED}} I_{\mathrm{H}} + I_2) V_t \ln(1 + \frac{\eta h P_{\mathrm{LED}} I_{\mathrm{H}} + I_2}{I_0}), \gamma'_1 \leq \frac{(\eta h P_{\mathrm{LED}} \frac{I_{\mathrm{H}}-I_{\mathrm{L}}}{2})^2}{P_{\mathrm{I}}(\Psi_{\mathrm{fov},1}) + \sigma^2},$$
$$0 \leq T \leq 1, \Psi_{\mathrm{fov}} \in \{\Psi_{\mathrm{fov}}^{[1]}, .., \Psi_{\mathrm{fov}}^{[M]}\} \Bigg\}, \tag{22}$$

$$\mathcal{C}_{\mathrm{R-E-}\gamma}^{\mathrm{TSBO}} \triangleq \bigcup_{T,A_1,B_1,\Psi_{\mathrm{fov},1}} \Bigg\{ (R', E'_{\mathrm{TSBO}}, \gamma'_1) : R' \leq T \log_2 \left(1 + \frac{(e\eta h P_{\mathrm{LED}} A_1)^2}{2\pi \left(P_{\mathrm{I}}(\Psi_{\mathrm{fov},1}) + \sigma^2 \right)} \right), E'_{\mathrm{TSBO}} \leq fT(\eta h P_{\mathrm{LED}} B_1 + I_2) \times$$
$$V_t \ln(1 + \frac{\eta h P_{\mathrm{LED}} B_1 + I_2}{I_0}) + f(1-T)(\eta h P_{\mathrm{LED}} I_{\mathrm{H}} + I_2) V_t \ln(1 + \frac{\eta h P_{\mathrm{LED}} I_{\mathrm{H}} + I_2}{I_0}), \gamma'_1 \leq \frac{(\eta h P_{\mathrm{LED}} A_1)^2}{P_{\mathrm{I}}(\Psi_{\mathrm{fov},1}) + \sigma^2},$$
$$0 \leq T \leq 1, A_1 \leq \min(B_1 - I_{\mathrm{L}}, I_{\mathrm{H}} - B_1), I_{\mathrm{L}} \leq B_1 \leq I_{\mathrm{H}}, \Psi_{\mathrm{fov}} \in \{\Psi_{\mathrm{fov}}^{[1]}, .., \Psi_{\mathrm{fov}}^{[M]}\} \Bigg\}. \tag{23}$$

Consequently, Proposition 1 has been proved by contradiction. ■

The optimal value $\Psi_{\mathrm{fov},1}$ is calculated similarly to the solution of (24). Regarding the rest optimization variables of (28) they are optimized according to the following theorem:

Theorem 2: For a specific value of $\Psi_{\mathrm{fov},1}$, the optimal value of T is given by

$$T^* = \underset{K_1 \leq T \leq K_2}{\operatorname{argmax}} \tilde{E}_{\mathrm{TSBO}} \tag{32}$$

with $\tilde{E}_{\mathrm{TSBO}}$ being solely a function of T and given by (20), by replacing A_1 and B_1 by

$$A_1 = \frac{1}{nhP_{\mathrm{LED}}} \sqrt{\frac{2\pi(P_{\mathrm{I}}(\Psi_{\mathrm{fov},1}) + \sigma^2)(2^{\frac{R_{\mathrm{th}}}{T}} - 1)}{e}}, \tag{33}$$

and

$$B_1 = I_{\mathrm{H}} - A_1, \tag{34}$$

respectively. Also,

$$K_1 = \frac{R_{\mathrm{th}}}{\log_2 \left(1 + \frac{e(\eta h_1 P_{\mathrm{LED}}(I_{\mathrm{H}} - I_{\mathrm{L}}))^2}{8\pi \left(P_{\mathrm{I}}(\Psi^*_{\mathrm{fov},1}) + \sigma^2 \right)} \right)} \tag{35}$$

$$K_2 = \min \left(\frac{R_{\mathrm{th}}}{\log_2 \left(1 + \frac{e\gamma_{\mathrm{th}}}{2\pi} \right)}, 1 \right). \tag{36}$$

Finally, the optimal values of A_1 and B_1 are given by (33) and (34), by replacing $\Psi_{\mathrm{fov},1}$ and T by $\Psi^*_{\mathrm{fov},1}$ and T^*, respectively.

Proof: Considering Proposition 1 and for a specific value of $\Psi_{\mathrm{fov},1}$ the optimization problem in (28) can be re-formulated as

$$\begin{aligned} \underset{B_1,A_1,T}{\mathbf{max}} \quad & E_{\mathrm{TSBO}} \\ \mathbf{s.t.} \quad & \mathrm{C}_1 : R \geq R_{\mathrm{th}}, \\ & \mathrm{C}_2 : \gamma_1 \geq \gamma_{\mathrm{th}}, \\ & \mathrm{C}_3 : A_1 + B_1 \leq I_{\mathrm{H}}, \\ & \mathrm{C}_4 : 0 \leq T \leq 1, \\ & \mathrm{C}_5 : A_1 \geq 0, \\ & \mathrm{C}_6 : B_1 \geq \tfrac{I_{\mathrm{H}}+I_{\mathrm{L}}}{2}. \end{aligned} \tag{37}$$

The optimization problem in (37) still cannot be easily solved in its current form, since the objective function as well as the constraints C_1 and C_2 are not concave. However, it can be solved with low complexity by using the following reformulation.

First, the inequalities in C_1 and C_3 are replaced by equalities. Then, A_1 and B_1 are given by (33) and (34), respectively. By substituting T_1 and B_1 by (33) and (34), C_1, C_3, and C_3 of (37) vanish, and the optimization problem is rewritten as

$$\begin{aligned} \underset{B_1,A,T_1 \forall n}{\mathbf{max}} \quad & \tilde{E}_{\mathrm{TSBO}} \\ \mathbf{s.t.} \quad & \mathrm{C}_2 : T \leq \tfrac{R_{\mathrm{th}}}{\log_2 \left(1 + \frac{e\gamma_{\mathrm{th}}}{2\pi} \right)}, \\ & \mathrm{C}_4 : 0 \leq T \leq 1, \\ & \mathrm{C}_6 : T \geq \tfrac{R_{\mathrm{th}}}{\log_2 \left(1 + \frac{e\left(\eta h_1 P_{\mathrm{LED}}(I_{\mathrm{H}} - I_{\mathrm{L}})\right)^2}{8\pi \left(P_{\mathrm{I}} + \sigma^2 \right)} \right)}, \end{aligned} \tag{38}$$

which is equivalent to (32), and, thus, the proof is completed. ■

V. Simulations and Discussion

We assume the downlink SLIPT system of Fig. 2, where the transmitter plane is parallel to the receiver one, i.e., $\varphi = \psi$. In the same room there are N other LEDs, which simultaneously use the same frequency band. The distance between each of them and from the dedicated LED is denoted by D.

TABLE II
Simulation parameters [30].

Parameter	Value	Parameter	Value
d	1.5 m	I_0	10^{-9} A
ψ	0	I_{L}	0 A
η	0.4 A/W	I_{H}	12 mA
f	0.75	T_{s}	1
P_{LED}	20 W/A	ρ	1.5
$\Phi_{1/2}$	60 deg	γ_{th}	10 dB
L_{r}	0.04 m^2	Ψ_{fov}	$\in \{30, 50\}$ deg
σ^2	10^{-15}	V_{t}	25 mV
D	1.5 m		

This article has been accepted for publication in a future issue of this journal, but has not been fully edited. Content may change prior to final publication. Citation information: DOI 10.1109/TGCN.2018.2818325, IEEE Transactions on Green Communications and Networking

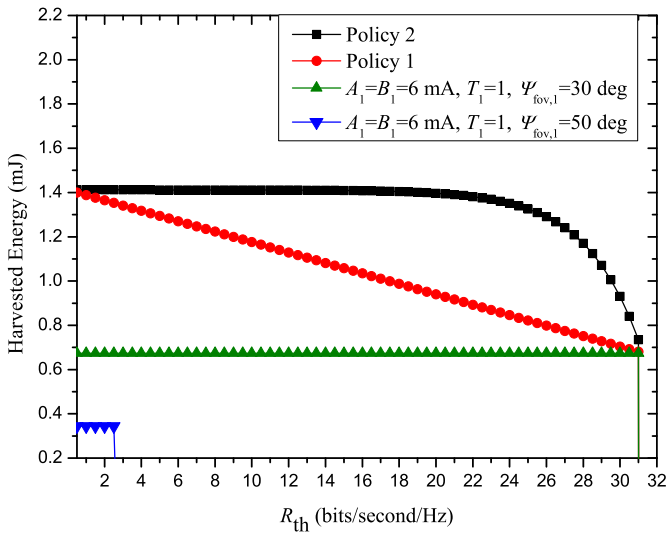

Fig. 3. Harvested energy vs R_{th} for $N = 1$.

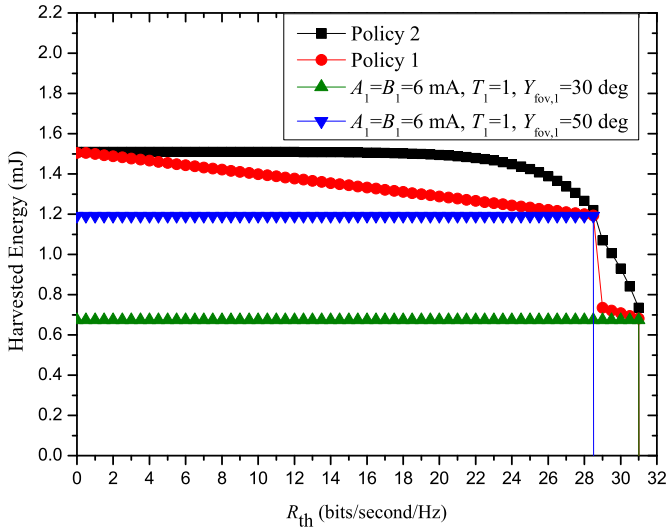

Fig. 4. Harvested energy vs R_{th} for $N = 1$.

Regarding the neighboring LEDs, we assume that the DC bias and the peak amplitude are denoted by A'_n and B'_n mA, $n \in \{1, ..., N\}$, respectively with $A'_n = B'_n$, while the rest parameters are equal to those of the dedicated LED. Furthermore, the channel between them and the user's receiver, denoted by h_n is modeled according to (3), using the corresponding parameters. Thus, when the widest FoV setting is selected, P_1 and I_2 are given by

$$P_1 = \sum_{n=1}^{N} (\eta h_n P_{\text{LED}} A'_n)^2 \tag{39}$$

and

$$I_2 = \sum_{n=1}^{N} \eta h_n P_{\text{LED}} B'_n, \tag{40}$$

otherwise their values are zero. Unless stated otherwise, the simulation parameters are given by Table II.

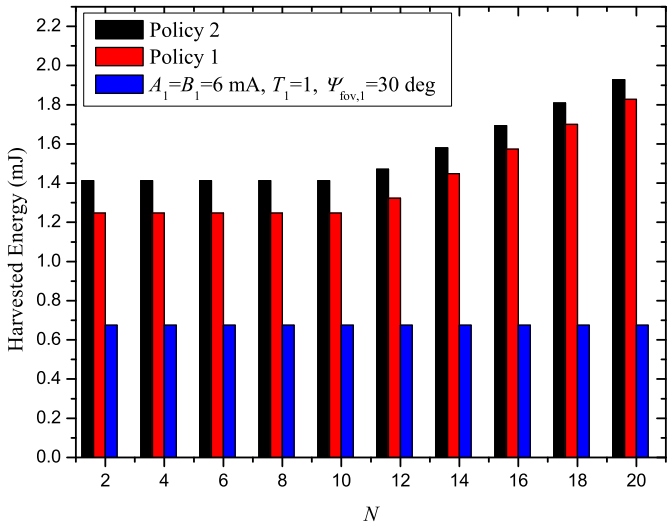

Fig. 5. Harvested energy vs N for $R_{th} = 7$ bits/second/Hz.

In Fig. 3. the performance of both optimized policies of Section III-C are compared for $N = 1$, $A'_n = 12$ mA, and $B'_n = 0$ A while they are also presented against the case of fixed A_1, B_1, T_1, and $\Psi_{\text{fov},1}$, which is considered as the baseline policy. More specifically, the harvested energy is plotted against the rate threshold. For this reason, the solutions of the optimization problems (24) and (28) have been used. The derived curves correspond to the rate-energy boundaries achieved by both optimized policies of Section III-C, which are given in (22) and (23), for $\gamma'_1 \geq \gamma_{\text{th}}$. As it is observed, both policies significantly outperform the baseline for both values of $\Psi_{\text{fov},1}$. Regarding the baseline, the value $\Psi_{\text{fov},1} = 50$ deg reduces the harvested energy compared to $\Psi_{\text{fov},1} = 30$ deg, because $g(\psi)$ decreases and thus, cancels the benefit of receiving the beam of the neighboring LED. For this reason, in this case case, none of the policies prefer the widest FoV setting. Also, the baseline policy with $\Psi_{\text{fov},1} = 50$ deg is infeasible for medium and high values of R_{th}, because the rate threshold cannot be reached, due to the received interference. Interestingly, Policy 2 outperforms Policy 1, especially for the high region of R_{th}, which is due to the extra degrees of freedom.

On the other hand, as it is observed by Fig. 4, which is for $N = 6$, $A'_n = 12$ mA, and $B'_n = 0$ A, in comparison to Fig. 3, as the energy that can be harvested by neighboring LEDs increases, the receiver tends to prefer the widest option, especially during phase 1, when the proposed policies are applied. This is because this setting leads to a considerably higher amount of harvested energy, which is also verified by noticing that the baseline policy with $\Psi_{\text{fov},1} = 50$ deg is now superior to the baseline policy with $\Psi_{\text{fov},1} = 30$ deg, as long as it is feasible. Also, it is noticed that the harvested energy is not continuous for the whole range of the required rate. The reason for this is that, when the rate requirement is small, the receiver prefers the widest FoV setting for both phases. However, as the rate requirement increases, the receiver prefers the smallest FoV setting for the second phase.

Similar conclusions can be obtained by Fig. 5, where the

harvested energy is plotted against the number of neighboring LEDS, for $A'_n = 6$ mA, and $B'_n = 6$ mA. For this specific setup, the baseline with $\Psi_{\text{fov},1} = 50$ deg is not feasible, and, thus, it is omitted. We notice here that for a small number of neighboring LEDs, the harvested energy remains constant, since the receiver prefers the smallest FoV setting. However, as the number of neighboring LEDs increases, the receiver prefers the widest FoV setting and the harvested energy increases with the increase of LEDs.

VI. Conclusions

In this paper, we have proposed and optimized new strategies and policies in order to balance the trade-off between the harvested energy and the QoS, when SLIPT with a solar panel based receiver is utilized. Considering that only the DC component can be used for energy harvesting, in contrast to AC component, which carries the information, the proposed optimization framework has focused on the appropriate selection of the DC bias, FoV, as well as the time dedicated solely to energy harvesting. The presented simulation results have verified that the proposed strategies considerably increase the harvested energy, compared to SLIPT with fixed policies. It is worth-noting that SLIPT creates a vast number of challenges and future research directions, such as the investigation of performance of specific types of solar cells (e.g., organic) and the utilization of separate receivers for information reception and energy harvesting.

References

[1] M. Ayyash, H. Elgala, A. Khreishah, V. Jungnickel, T. Little, S. Shao, M. Rahaim, D. Schulz, J. Hilt, and R. Freund, "Coexistence of WiFi and LiFi toward 5G: Concepts, Opportunities, and Challenges," *IEEE Commun. Mag.*, vol. 54, no. 2, pp. 64–71, Feb. 2016.

[2] M. S. A. Mossaad, S. Hranilovic, and L. Lampe, "Visible Light Communications Using OFDM and Multiple LEDs," *IEEE Trans. Commun.*, vol. 63, no. 11, pp. 4304–4313, Nov. 2015.

[3] M. Kavehrad, "Sustainable Energy-Efficient Wireless Applications Using Light," *IEEE Commun. Mag.*, vol. 48, no. 12, pp. 66–73, Dec. 2010.

[4] S. Arnon, Ed., *Visible Light Communication*. Cambridge University Press, 2015.

[5] D. Bykhovsky and S. Arnon, "Multiple Access Resource Allocation in Visible Light Communication Systems," *J. Lightw. Technol.*, vol. 32, no. 8, pp. 1594–1600, Apr. 2014.

[6] S. Sudevalayam and P. Kulkarni, "Energy Harvesting Sensor Nodes: Survey and Implications," *IEEE Commun. Surveys Tuts.*, vol. 13, no. 3, pp. 443–461, Jul. 2010.

[7] P. D. Diamantoulakis, "Resource Allocation in Wireless Networks with Energy Constraints," Ph.D. dissertation, Aristotle University of Thessaloniki, Thessaloniki, Greece, 2017.

[8] P. D. Diamantoulakis, K. N. Pappi, Z. Ding, and G. K. Karagiannidis, "Wireless-Powered Communications with Non-Orthogonal Multiple Access," *IEEE Trans. Wireless Commun.*, vol. 15, no. 12, pp. 8422–8436, Dec. 2016.

[9] Q. Liu, J. Wu, P. Xia, S. Zhao, W. Chen, Y. Yang, and L. Hanzo, "Charging Unplugged: Will Distributed Laser Charging for Mobile Wireless Power Transfer Work?" *IEEE Veh. Technol. Mag.*, vol. 11, no. 4, pp. 36–45, Dec. 2016.

[10] C. C. M. Kyba, T. Kuester, A. Sánchez de Miguel, K. Baugh, A. Jechow, F. Hölker, J. Bennie, C. D. Elvidge, K. J. Gaston, and L. Guanter, "Artificially Lit Surface of Earth at Night Increasing in Radiance and Extent," *Science Advances*, vol. 3, no. 11, 2017.

[11] I. Krikidis, S. Timotheou, S. Nikolaou, G. Zheng, D. W. K. Ng, and R. Schober, "Simultaneous Wireless Information and Power Transfer in Modern Communication Systems," *IEEE Commun. Mag.*, vol. 52, no. 11, pp. 104–110, Nov. 2014.

[12] P. Grover and A. Sahai, "Shannon Meets Tesla: Wireless Information and Power Transfer," in *IEEE International Symposium on Information Theory*, Jun. 2010, pp. 2363–2367.

[13] L. R. Varshney, "Transporting Information and Energy Simultaneously," in *IEEE International Symposium on Information Theory*, Jul. 2008, pp. 1612–1616.

[14] R. Zhang and C. K. Ho, "MIMO Broadcasting for Simultaneous Wireless Information and Power Transfer," in *2011 IEEE Global Telecommunications Conference - GLOBECOM 2011*, Dec. 2011, pp. 1–5.

[15] ——, "MIMO Broadcasting for Simultaneous Wireless Information and Power Transfer," *IEEE Trans. Wireless Commun.*, vol. 12, no. 5, pp. 1989–2001, May 2013.

[16] L. R. Varshney, "Unreliable and Resource-Constrained Decoding," Ph.D. dissertation, Massachusetts Institute of Technology, Jun 2010.

[17] X. Zhou, R. Zhang, and C. K. Ho, "Wireless Information and Power Transfer: Architecture Design and Rate-Energy Tradeoff," *IEEE Trans. Commun.*, vol. 61, no. 11, pp. 4754–4767, Nov. 2013.

[18] L. Liu, R. Zhang, and K. C. Chua, "Wireless Information Transfer with Opportunistic Energy Harvesting," *IEEE Trans. Wireless Commun.*, vol. 12, no. 1, pp. 288–300, Jan. 2013.

[19] P. D. Diamantoulakis, K. N. Pappi, G. K. Karagiannidis, H. Xing, and A. Nallanathan, "Joint Downlink/Uplink Design for Wireless Powered Networks with Interference," *IEEE Access*, vol. 5, pp. 1534–1547, Jan. 2017.

[20] S. Nikoletseas, Y. Yang, and A. Georgiadis, Eds., *Wireless Power Transfer Algorithms, Technologies and Applications in Ad Hoc Communication Networks*. Springer, 2016.

[21] J. Fakidis, S. Videv, S. Kucera, H. Claussen, and H. Haas, "Indoor Optical Wireless Power Transfer to Small Cells at Nighttime," *J. Lightw. Technol.*, vol. 34, no. 13, pp. 3236–3258, Jul. 2016.

[22] C. Carvalho and N. Paulino, "On the Feasibility of Indoor Light Energy Harvesting for Wireless Sensor Networks," *Procedia Technology*, vol. 17, pp. 343–350, 2014.

[23] A. Nasiri, S. A. Zabalawi, and G. Mandic, "Indoor Power Harvesting using Photovoltaic Cells for Low-Power Applications," *IEEE Trans. Ind. Electron.*, vol. 56, no. 11, pp. 4502–4509, Nov. 2009.

[24] G. Pan, J. Ye, and Z. Ding, "Secure Hybrid VLC-RF Systems with Light Energy Harvesting," *IEEE Trans. Commun.*, vol. 65, no. 10, pp. 4348–4359, Oct. 2017.

[25] Y. Li, N. Huang, J. Wang, Z. Yang, and W. Xu, "Sum Rate Maximization for VLC Systems with Simultaneous Wireless Information and Power Transfer," *IEEE Photon. Technol. Lett.*, vol. 29, no. 6, pp. 531–534, Mar. 2017.

[26] Z. Wang, D. Tsonev, S. Videv, and H. Haas, "Towards Self-Powered Solar Panel Receiver for Optical Wireless Communication," in *Proc. IEEE International Conference on Communications (ICC)*, Jun. 2014, pp. 3348–3353.

[27] ——, "On the Design of a Solar-Panel Receiver for Optical Wireless Communications with Simultaneous Energy Harvesting," *IEEE J. Sel. Areas Commun.*, vol. 33, no. 8, pp. 1612–1623, Aug. 2015.

[28] H. Sandalidis, A. Vavoulas, T. Tsiftsis, and N. Vaiopoulos, "Illumination, Data Transmission and Energy Harvesting: The Threefold Advantage of VLC," 2017.

[29] X. Chen, C. Min, and J. Guo, "Visible Light Communication System Using Silicon Photocell for Energy Gathering and Data Receiving," *International Journal of Optics*, vol. 2017, 2017.

[30] T. Rakia, H. C. Yang, F. Gebali, and M. S. Alouini, "Optimal Design of Dual-Hop VLC/RF Communication System with Energy Harvesting," *IEEE Comm. Lett.*, vol. 20, no. 10, pp. 1979–1982, Oct. 2016.

[31] ——, "Dual-Hop VLC/RF Transmission System with Energy Harvesting Relay under Delay Constraint," in *Proc. IEEE Globecom Workshops*, Dec. 2016, pp. 1–6.

[32] T. Komine and M. Nakagawa, "Fundamental Analysis for Visible-Light Communication System Using LED Lights," *IEEE Trans. Consum. Electron.*, vol. 50, no. 1, pp. 100–107, Feb. 2004.

[33] H. Ma, L. Lampe, and S. Hranilovic, "Coordinated Broadcasting for Multiuser Indoor Visible Light Communication Systems," *IEEE Trans. Commun.*, vol. 63, no. 9, pp. 3313–3324, Sep. 2015.

[34] J. M. Kahn and J. R. Barry, "Wireless Infrared Communications," *Proc. IEEE*, vol. 85, no. 2, pp. 265–298, Feb. 1997.

[35] C. Li, W. Jia, Q. Tao, and M. Sun, "Solar Cell Phone Charger Performance in Indoor Environment," in *Proc. IEEE 37th Annual Northeast Bioengineering Conference (NEBEC)*, 2011, pp. 1–2.

[36] A. Al-Ghamdi and J. Elmirghani, "Performance and Field of View Optimization of an Optical Wireless Pyramidal Fly-Eye Diversity Receiver," *Journal of optical communications*, vol. 23, no. 6, pp. 215–222, 2002.

This article has been accepted for publication in a future issue of this journal, but has not been fully edited. Content may change prior to final publication. Citation information: DOI 10.1109/TGCN.2018.2818325, IEEE Transactions on Green Communications and Networking

[37] Y. S. Tsou, Y. H. Lin, and A. C. Wei, "Concentrating Photovoltaic System using a Liquid Crystal Lens," *IEEE Photon. Technol. Lett.*, vol. 24, no. 24, pp. 2239–2242, Dec. 2012.
[38] J. B. Wang, Q. S. Hu, J. Wang, M. Chen, and J. Y. Wang, "Tight Bounds on Channel Capacity for Dimmable Visible Light Communications," *J. Lightw. Technol.*, vol. 31, no. 23, pp. 3771–3779, Dec. 2013.

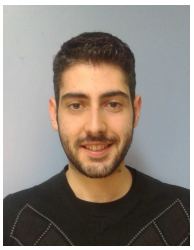

Panagiotis D. Diamantoulakis (S'13-M'17) was born in Thessaloniki, Greece, in 1989. He received the Diploma Degree (5 years) and his PhD in Electrical and Computer Engineering from the Aristotle University of Thessaloniki, Greece, in 2012 and 2017, respectively. His current research interests include wireless communications, wireless power transfer, optical wireless communications, optimization theory and applications, and game theory.

During 2014-2016, he was a visitor researcher at the department of Electrical and Computer Engineering at Khalifa University, UAE, and at the Institute for Digital Communications (IDC) of the Telecommunications Laboratory (LNT) at Friedrich-Alexander-Universität Erlangen-Nürnberg (FAU), Germany. In 2015, he received the student travel grant for the International Workshop on Optical Wireless Communication (IWOW), Istanbul, Turkey.

He is co-author of a chapter titled Trade-offs in Wireless Powered Communications, in the book Wireless Power Transfer Algorithms, Technologies and Applications in Ad Hoc Communication Networks, Springer, 2017. He is Editor of *Journal of Communications and Information Networks* and Guest Editor of *Applied Sciences* for the Special Issue Optical Wireless Communications. He was Member of the International Advisory Committee in the *International Conference on Big Data and Data Analytics (ICBDDA-17)*. He has served as a reviewer in various IEEE journals and conferences and as member of the technical program committee of various international IEEE and non-IEEE conferences. Also, he was an exemplary reviewer (top 3% of reviewers) in *IEEE Communication Letters* and *IEEE Transactions on Wireless Communications*, for 2014 and 2017, respectively.

George K. Karagiannidis (M'96-SM'03-F'14) was born in Pithagorion, Samos Island, Greece. He received the University Diploma (5 years) and PhD degree, both in electrical and computer engineering from the University of Patras, in 1987 and 1999, respectively. From 2000 to 2004, he was a Senior Researcher at the Institute for Space Applications and Remote Sensing, National Observatory of Athens, Greece. In June 2004, he joined the faculty of Aristotle University of Thessaloniki, Greece where he is currently Professor in the Electrical & Computer Engineering Dept. and Director of Digital Telecommunications Systems and Networks Laboratory. He is also Honorary Professor at South West Jiaotong University, Chengdu, China.

His research interests are in the broad area of Digital Communications Systems and Signal processing, with emphasis on Wireless Communications, Optical Wireless Communications, Wireless Power Transfer and Applications, Molecular and Nanoscale Communications, Stochastic Processes in Biology and Wireless Security. He is the author or co-author of more than 450 technical papers published in scientific journals and presented at international conferences. He is also author of the Greek edition of a book on Telecommunications Systems and co-author of the book Advanced Optical Wireless Communications Systems, Cambridge Publications, 2012.

Dr. Karagiannidis has been involved as General Chair, Technical Program Chair and member of Technical Program Committees in several IEEE and non-IEEE conferences. In the past, he was Editor in IEEE Transactions on Communications, Senior Editor of *IEEE Communications Letters*, Editor of the *EURASIP Journal of Wireless Communications & Networks* and several times Guest Editor in *IEEE Selected Areas in Communications*. From 2012 to 2015 he was the Editor-in Chief of *IEEE Communications Letters*.

Dr. Karagiannidis is IEEE Fellow and one of the highly-cited authors across all areas of Electrical Engineering, recognized as 2015, 2016 and 2017 Web-of-Science Highly-Cited Researcher.

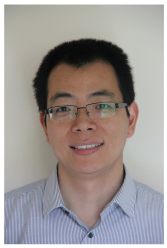

Zhiguo Ding (S'03-M'05) received his B.Eng in Electrical Engineering from the Beijing University of Posts and Telecommunications in 2000, and the Ph.D degree in Electrical Engineering from Imperial College London in 2005. From Jul. 2005 to Aug. 2014, he was working in Queen's University Belfast, Imperial College and Newcastle University. Since Sept. 2014, he has been with Lancaster University as a Chair Professor. From Oct. 2012 to Sept. 2019, he has also been an academic visitor in Princeton University.

Dr Ding' research interests are 5G networks, game theory, cooperative and energy harvesting networks and statistical signal processing. He is serving as an Editor for *IEEE Transactions on Communications*, *IEEE Transactions on Vehicular Technology*, and *Journal of Wireless Communications and Mobile Computing*, and was an Editor for *IEEE Wireless Communication Letters*, *IEEE Communication Letters* from 2013 to 2016. He received the best paper award in IET Comm. Conf. on Wireless, Mobile and Computing, 2009, IEEE Communication Letter Exemplary Reviewer 2012, and the EU Marie Curie Fellowship 2012-2014.